

Supporting Information

Hydrothermal synthesis of ordered mesoporous carbons from  
biomass-derived precursor for electrochemical capacitors

Shanshan Feng,<sup>a</sup> Wei Li,<sup>a</sup> Jinxiu Wang,<sup>a</sup> Yanfang Song,<sup>a</sup> Ahmed A. Elzatahry,<sup>b</sup>  
Yongyao Xia<sup>a</sup> and Dongyuan Zhao\*<sup>a</sup>

<sup>a</sup> Department of Chemistry, Laboratory of Advanced Materials, Shanghai Key Lab of Molecular Catalysis and Innovative Materials, and State key Laboratory of Molecular Engineering of Polymers, Fudan University, Shanghai 200433, P. R. China. Tel: (+86) 21-5163-0205, Fax: (+86) 21-5163-0307

E-mail: [dyzhao@fudan.edu.cn](mailto:dyzhao@fudan.edu.cn).

<sup>b</sup> Department of Chemistry-College of Science, King Saud University, Riyadh 11451, Saudi Arabia; Polymer Materials Research Department, Advanced Technology and New Materials Research Institute, City of Scientific Research and Technology Applications, New Borg El-Arab City, Alexandria 21934, Egypt.

## Experimental Section

**Chemicals.** Triblock poly(ethylene oxide)-*b*-poly(propyleneoxide)-*b*-poly(ethylene oxide) copolymers Pluronic P123 (EO<sub>20</sub>PO<sub>70</sub>EO<sub>20</sub>,  $M_{av} = 5800$ ) and Pluronic F127 (EO<sub>106</sub>PO<sub>70</sub>EO<sub>106</sub>,  $M_{av} = 12600$ ) were purchased from Aldrich. Hydrochloric acid was obtained from Sinopharm Chemical Reagent Co., Ltd. (China).  $\beta$ -cyclodextrins was purchased from Aladdin. Deionized water was used for all experiment. All chemicals were used as received without further purification.

**Synthesis of ordered mesoporous carbons (OMCs).** The ordered mesoporous carbons were fabricated by the soft-templating strategy *via* a hydrothermal carbonization route. In a typical synthesis, 2 M HCl aqueous solution (1 mL) was mixed with a aqueous solution of mixed Pluronic PEO-PPO-PEO (0.75 g of P123 and 1.25 g of F127 in 20 mL of H<sub>2</sub>O). Subsequently, 2.0 g of  $\beta$ -cyclodextrins (denoted as  $\beta$ -CD) was added under stirring, then transferred to a 40-mL Teflon-lined stainless steel autoclave, and hydrothermally treated for 36 h at 140 °C. After cooling down, the solid product was obtained. Carbonization was carried out in a tubular furnace at 700 °C for 3 h under a N<sub>2</sub> flow, the heating rate was set as 1 °C/min.

**Electrochemical measurements.** The working electrodes were assembled on nickel foam collectors. A mixture of 80 wt% activated samples, 10 wt% acetylene black, and 10 wt% polytetrafluoroethylene (PTFE) was dispersed in alcohol and pressed on nickel foam under 20 MPa. Then, the electrodes were dried at 100 °C for 12 h. The

typical mass load of the electrode was 5 mg/cm<sup>2</sup>. The electrochemical performances of the prepared electrodes were characterized by cyclic voltammetry (CV) and charge–discharge tests. 6.0 M KOH solution was used as the electrolyte. The experiments were carried out using a three-electrode cell under the potential window of -0.1 ~ -0.9 V, in which platinum and Hg/HgO electrodes (in 6.0 M KOH) were used as counter and reference electrodes, respectively. The experiments were performed on an electrochemical analyzer (CHI 760) under ambient conditions.

### ***Materials Characterization.***

Transmission electron microscopy (TEM) experiments were conducted on a JEOL JEM-2100 F microscope (Japan) operated at 200 kV. The samples for the TEM measurements were suspended in ethanol and supported onto a holey carbon film on a Cu grid. Field-emission scanning electron microscopy (FESEM) images were taken on a Hitachi S-4800 microscope. Nitrogen sorption isotherms were measured at 77 K with a Micromeritics Tristar 2420 analyzer (USA). Before measurements, the samples were degassed in a vacuum at 180 °C for at least 6 h. The Brunauer-Emmett-Teller (BET) method was utilized to calculate the specific surface areas. The pore size distributions (PSD) were derived from the adsorption branch of the isotherms using the Barrett-Joyner-Halenda (BJH) model and non-local density functional theory (NLDFT) model for cylinder pore geometry, respectively. The total pore volume  $V_t$  was estimated from the adsorbed amount at a relative pressure  $P/P_0$  of 0.995. The micropore volume ( $V_m$ ) and micropore surface area ( $V_{\text{micro}}$ ) were calculated from the

$V_t$  plot method. Small-angle X-ray scattering (SAXS) measurements were taken on a Nanostar U small-angle X-ray scattering system (Bruker, Germany) using Cu  $K\alpha$  radiation (40 kV, 35 mA). The  $d$ -spacing values were calculated by the formula  $d = 2\pi/q$ , wherein  $q$  is the scattering vector. X-ray diffraction (XRD) patterns were recorded on a D8 advance X-ray diffractometer (Bruker, Germany) with Ni-filtered Cu  $K\alpha$  radiation (40 kV, 40 mA). Fourier transform infrared (FT-IR) spectra were measured on an IR Prestige-21 spectrometer (Shimadzu, Japan) using KBr disks of the solid samples. Raman spectra were collected by using Raman microscopes (Renishaw, UK) under 630 nm excitation.

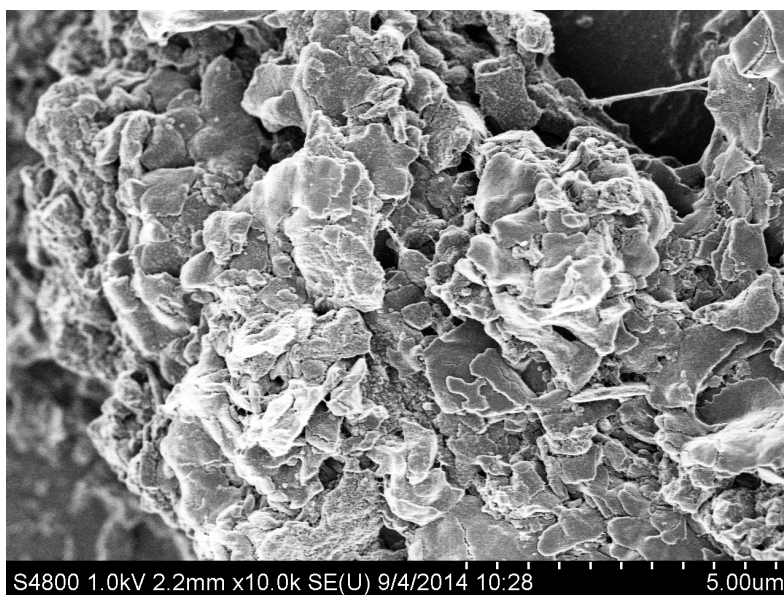


**Fig. S1** Field-emission scanning electron microscopy (FESEM) image of the ordered mesoporous carbons (OMCs) derived from  $\beta$ -CD as a carbon source after hydrothermal treatment and carbonized at 700 °C.

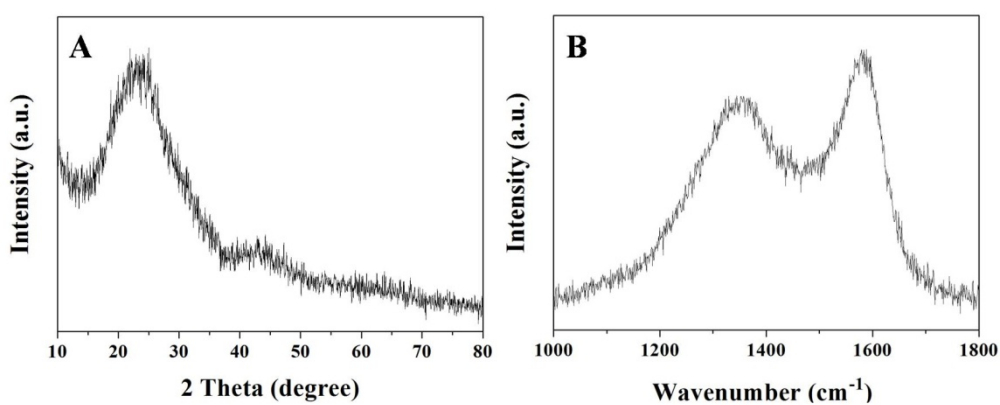


**Fig. S2** XRD pattern (A) and Raman spectra (B) of the ordered mesoporous carbons carbonized at 700 °C.

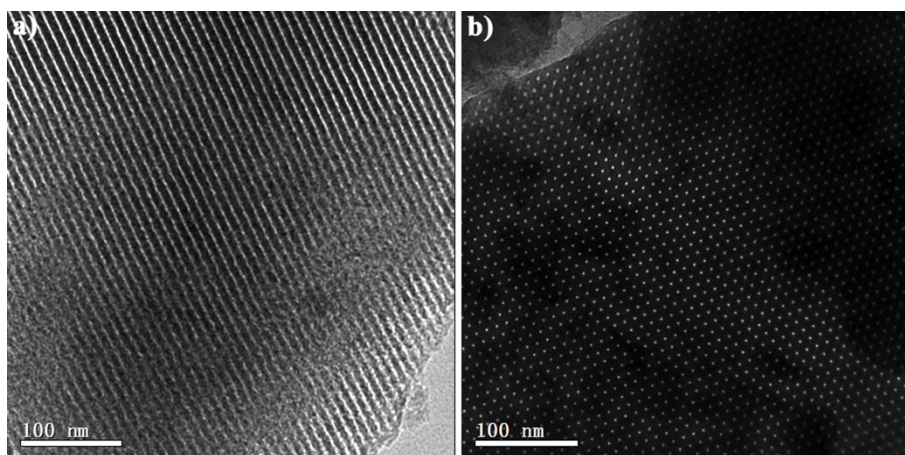


**Fig. S3** TEM images of the mesoporous carbon FDU-15 derived from phenolic-resins carbonized at 700 °C viewed from the [11] (a) and [10] (b) directions, respectively.

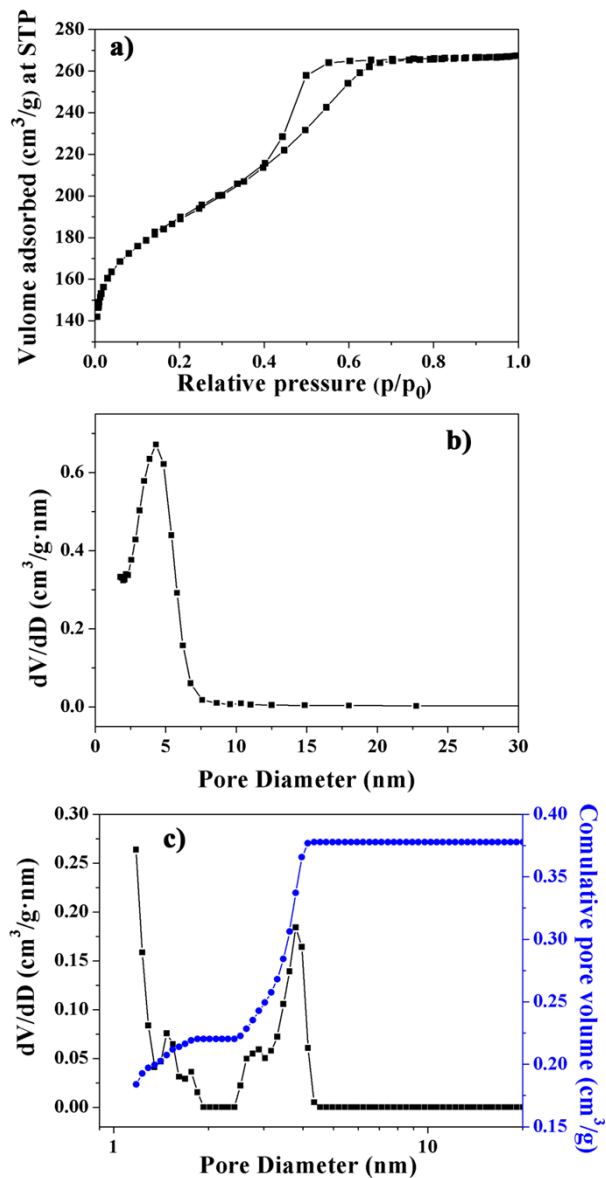


**Fig. S4** (a)  $\text{N}_2$  sorption isotherms, (b) the corresponding pore size distribution curve using the Barrett-Joyner-Halenda (BJH) model, and (c) the corresponding pore size distribution curve using non-local density functional theory (NLDFT) model and cumulative pore volume curve of the mesoporous carbon FDU-15 derived from phenolic-resins after carbonized at  $700\text{ }^\circ\text{C}$ .

Table S1. Textural properties comparison of the ordered mesoporous carbons derived from  $\beta$ -CD and various OMCs derived from phenolic-resins.

Carbon precursor	Carbonization temperature (°C)	$S_{BET}$ (m <sup>2</sup> /g)	$S_{Micro}$ (m <sup>2</sup> /g)	$V_{total}$ (cm <sup>3</sup> /g)	$V_{micro}$ (cm <sup>3</sup> /g)	$S_{Micro}/S_{BE}$ <sub>T</sub> (%)	Ref
<b><math>\beta</math>-CD</b>	<b>700</b>	<b>781</b>	<b>579</b>	<b>0.41</b>	<b>0.27</b>	<b>74</b>	
Resol	700	627	326	0.44		52	1
Resol	700	660	180	0.44	0.07	27	2
Resol	700	750	430	0.42		57	3
R-F	800	667	395	0.63	0.14	59	4
R-F	850	607		0.58			5
Resol	900	650	350	0.37		54	6
Resol	900	1270	72	4.3		5.7	7
PS	1000	1504	123	2.62	0.054	8.2	8
Resol	900	746	406	0.41	0.19	54	9
R-F	800	694	264	0.66	0.16	38	10
P-F	900	990	257	0.86		26	11
R-F	600	758	405		0.16	53	12
R-HMT	700	820	423	0.59		52	13

R-F: Resorcinol and Formaldehyde

P-F: Phenol and Formaldehyde

PS: Polystyrene

R-HMT: Resorcinol and Hexamine



**Table S2.** Textural properties of the ordered mesoporous carbons derived from  $\beta$ -CD and FDU-15 derived from phenolic-resins after carbonized at 700 °C.

Sample	$S_{BET}^a$ (m <sup>2</sup> /g)	$S_{micro}^b$ (m <sup>2</sup> /g)	$D_{BJH}^c$ (nm)	$D_{NLDFT}^d$ (nm)	$V_{total}^e$ (cm <sup>3</sup> /g)	$V_{micro}^f$ (cm <sup>3</sup> /g)	Specific capacitance (F/g)
OMCs	781	579	4.5	1.2/3.8	0.41	0.27	157
FDU-15	661	372	4.3	1.4/3.8	0.38	0.22	112

<sup>a</sup> Specific surface area estimated using BET method; <sup>b</sup> Micropore surface area calculated using the  $V_t$  plot method; <sup>c</sup> Pore size calculated using BJH model; <sup>d</sup> Pore size calculated using NLDFT method; <sup>e</sup> Total pore volume; <sup>f</sup> Micropore volume.

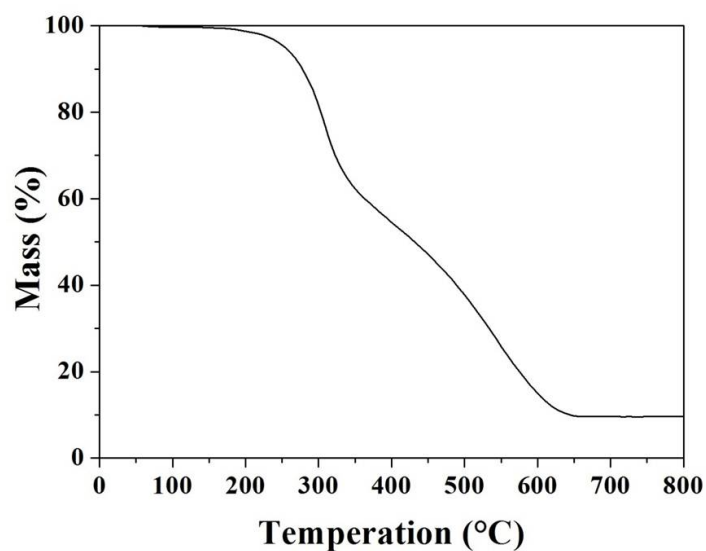


**Fig. S5** Thermogravimetric analysis (TGA) curve of the as-made ordered mesoporous carbons derived from  $\beta$ -CD as a carbon source *via* a hydrothermal process.

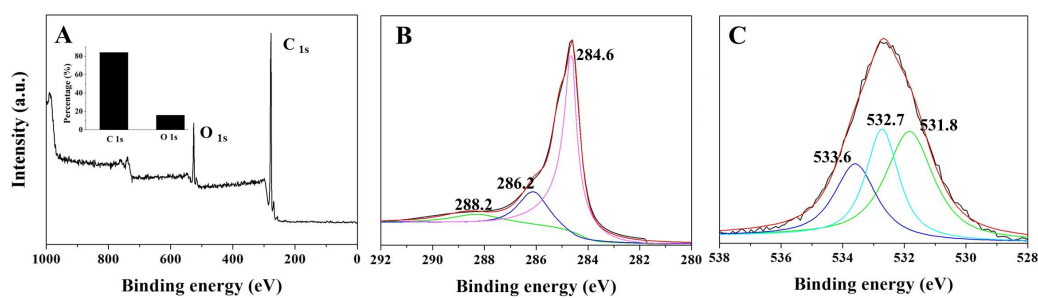


**Fig. S6** X-ray photoelectron spectra (XPS) of the ordered mesoporous carbons derived from  $\beta$ -CD as a carbon source after hydrothermal treatment and carbonized at 700 °C: A) the survey spectrum; B) high-resolution spectra of C 1s; C) high-resolution spectra of O 1s.

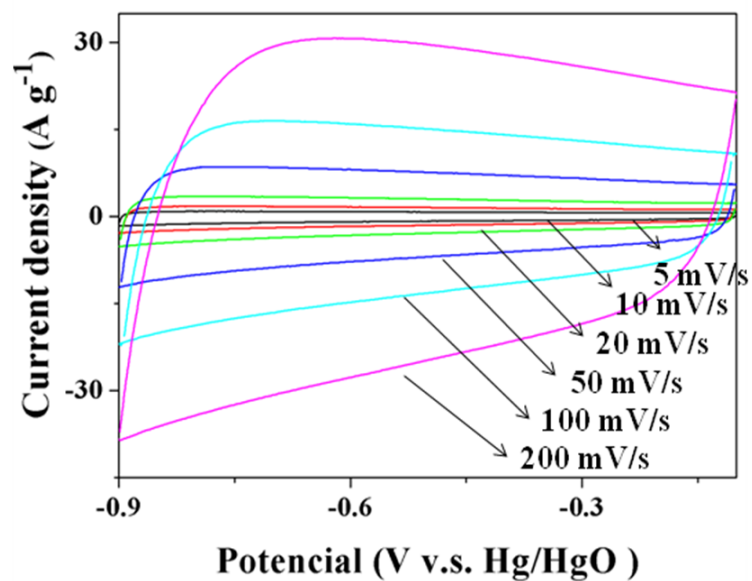


**Fig. S7** Capacitance–voltage cyclic curves for the OMCs at 700 °C at different potential rates of 5 – 200 mV/s.

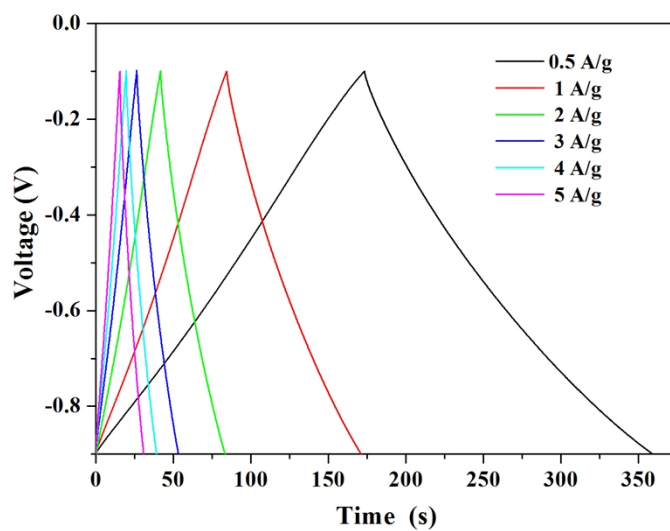


**Fig. S8** Galvanostatic charge/discharge curves of the mesoporous carbon FDU-15 at current densities of 0.5 – 5 A/g.

Table S3. The specific capacitance comparison of the ordered mesoporous carbons derived from  $\beta$ -CD and various OMCs derived from other precursor under the same electrolyte condition.

	$S_{BET}$ (m <sup>2</sup> /g)	$V_{total}$ (cm <sup>3</sup> /g)	Electrolyte	Current densities	Capacity (F/g)	Ref
<b><math>\beta</math>-CD</b>	<b>781</b>	<b>0.41</b>	<b>6 M KOH</b>	<b>0.5 A/g</b>	<b>157</b>	
Resol	627		6 M KOH	0.5 A/g	130	14
Resol	660	0.44	6 M KOH	0.5 A/g	130	15
Sucrose	984	1.09	6 M KOH	2 mV/s	115	16
Furfuryl alcohol	1880	1.08	6 M KOH	0.5 A/g	145	17
R-F	803	0.49	6 M KOH	1 A/g	116	18
Resol	700	0.46	6 M KOH	0.5 A/g	136	19

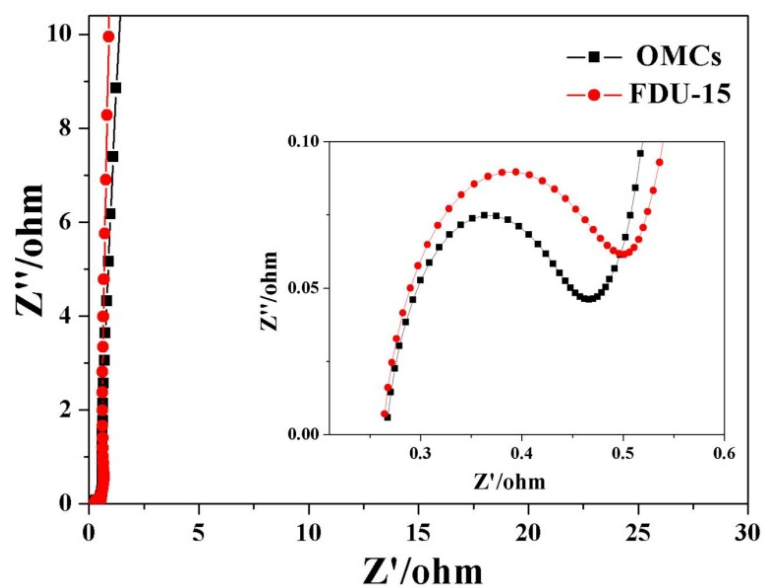


**Fig. S9** Nyquist plots of the ordered mesoporous carbons derived from  $\beta$ -CD and FDU-15 derived from phenolic-resins after carbonized at 700 °C. Inset shows a zoomed-in plot at a high frequency region.

## References

1. Wang, J.; Xue, C.; Lv, Y.; Zhang, F.; Tu, B.; Zhao, D. *Carbon* **2011**, *49*, 4580.
2. Lv, Y.; Zhang, F.; Dou, Y.; Zhai, Y.; Wang, J.; Liu, H.; Xia, Y.; Tu, B.; Zhao, D. *J. Mater. Chem.* **2012**, *22*, 93.
3. Meng, Y.; Gu, D.; Zhang, F.; Shi, Y.; Cheng, L.; Feng, D.; Wu, Z.; Chen, Z.; Wan, Y.; Stein, A.; Zhao, D. *Chem. Mater.* **2006**, *18*, 4447.
4. Chen, M.; Shao, L.-L.; Qian, X.; Liu, L.; Ren, T. Z.; Yuan, Z. Y. *Chem. Eng. J.* **2014**, *256*, 23.
5. Wang, X.; Liang, C.; Dai, S. *Langmuir* **2008**, *24*, 7500.

6. Li, H. Q.; Liu, R. L.; Zhao, D. Y.; Xia, Y. Y. *Carbon* **2007**, *45*, 2628.
7. Liu, H. J.; Wang, X. M.; Cui, W. J.; Dou, Y. Q.; Zhao, D. Y.; Xia, Y. Y. *J. Mater. Chem.* **2010**, *20*, 4223.
8. Woo, S. W.; Dokko, K.; Nakano, H.; Kanamura, K. *J. Mater. Chem.* **2008**, *18*, 1674.
9. Liang, Y.; Wu, D.; Fu, R. *Langmuir* **2009**, *25*, 7783.
10. Jin, J.; Tanaka, S.; Egashira, Y.; Nishiyama, N. *Carbon* **2010**, *48*, 1985.
11. Liang, Y.; Li, Z.; Fu, R.; Wu, D. *J. Mater. Chem. A* **2013**, *1*, 3768.
12. Liu, L.; Deng, Q. F.; Agula, B.; Ren, T. Z.; Liu, Y. P.; Zhaorigetu, B.; Yuan, Z. *Y. Catal. Today* **2012**, *186*, 35.
13. Liu, D.; Xia, L. J.; Qu, D.; Lei, J. H.; Li, Y.; Su, B. L. *J. Mater. Chem. A* **2013**, *1*, 15447.
14. Wang, J.; Xue, C.; Lv, Y.; Zhang, F.; Tu, B.; Zhao, D. *Carbon* **2011**, *49*, 4580.
15. Lv, Y.; Zhang, F.; Dou, Y.; Zhai, Y.; Wang, J.; Liu, H.; Xia, Y.; Tu, B.; Zhao, D. *J. Mater. Chem.* **2012**, *22*, 93.
16. Xia, K.; Gao, Q.; Jiang, J.; Hu, J. *Carbon* **2008**, *46*, 1718.
17. Fuertes, A. B.; Lota, G.; Centeno, T. A.; Frackowiak, E. *Electrochim. Acta* **2005**, *50*, 2799.
18. Xiong, W.; Liu, M.; Gan, L.; Lv, Y.; Li, Y.; Yang, L.; Xu, Z.; Hao, Z.; Liu, H.; Chen, L. *J. Power Sources* **2011**, *196*, 10461.
19. Feng, D.; Lv, Y.; Wu, Z.; Dou, Y.; Han, L.; Sun, Z.; Xia, Y.; Zheng, G.; Zhao, D. *J. Am. Chem. Soc.* **2011**, *133*, 15148.